Particle Accelerators
1981 Vol.11 pp.201–211
0031-2460/81/1104/0201$06.50/0

HEAD–TAIL INSTABILITY INDUCED BY A MATCHED KICKER MAGNET

YOSHIKAZU MIYAHARA

Synchrotron Radiation Laboratory, University of Tokyo, Tokyo, 188, Japan

(Received July 2, 1980; in final form March 4, 1981)

The head–tail instability of a bunched beam induced by a matched kicker magnet is examined experimentally and theoretically. A new theoretical approach to the instability with the use of a free-string model of the bunched beam and an appropriate analysis of the transient process of the induced current in the magnet allows us to develop a theory that gives quantitative agreement with the experimental results and agrees with the Pellegrini-Sands formula for the growth rate with small chromaticity.

INTRODUCTION

Coherent transverse instability of a bunched beam was first treated by Courant and Sessler[1] for a resistive-wall vacuum chamber. They considered a bunch-to-bunch interaction with a pencil model of the bunched beam. Pellegrini[2] and Sands[3] have succeeded in explaining the instability by taking into account an intrabunch interaction (the head–tail effect), which includes the coupling between betatron and synchrotron oscillations. Sacherer[4] gave a general formula for the instability and Gareyte and Sacherer[5] observed the dynamic motion of the bunched beam under the instability. According to the head-tail theory the instability is not to be induced for zero chromaticity of the machine. This is successfully applied to suppress the instability in many accelerators.

In spite of the excellent explanation of the instability, however, the theory has not achieved a quantitative agreement with experiments, especially in regard to the growth rate of the instability.[2,3] One of the reasons is ascribed to the complex calculation of the wake field induced by the beam in surrounding environments, vacuum chamber, rf cavity, pick-up electrode, and magnet. Accordingly, almost all recent efforts have been made for the investigation of the wake field or equivalent coupling impedance of the environments.[6–8]

In the KEK booster, a 500-MeV proton synchrotron, we have observed the coherent transverse instability in the horizontal direction. This is induced by the interaction of the beam with a ferrite-loaded kicker magnet.[9] In the ordinary operation the magnet is terminated with a matched resistance. The instability grows more rapidly when the resistance is removed. In a previous paper[10] we have successfully made a theoretical description of the instability induced by the unmatched kicker magnet with the use of a free string model of the bunched beam and on the basis of a detailed analysis of the induced current in the magnet. In this paper we examine the instability induced by a matched magnet. So far the harmfulness of kicker magnets has been noticed and the calculation and measurement have been made, but no satisfactory explanation of the instability.[6,11] A complicated theory of the instability induced by some matched surroundings was given by Derbenev et al.[12]

Characteristic features of the previous treatment are as follows. The interaction of the beam with the magnet is represented by the mutual inductance

$$M = a - bx, \tag{1-1}$$

where $a = 1.01 \times 10^{-7}$, $b = 1.60 \times 10^{-9}$, and x is the horizontal position of the beam current. The linear dependence of M on x, which is due to the C structure of the magnet, is responsible for the instability. The induced current becomes large when the betatron oscillation frequency of the beam meets the resonance frequency of the unmatched magent. The damping time of the induced current is comparable to the revolution

period, so that bunch-to-bunch interaction as well as intra-bunch interaction were taken into account with the use of Fourier expansion method.

In contrast, in the matched case the induced current does not make any resonance in the matched magnet but travels away quickly into the termination. Hence the interaction works only within a single bunch. It is important to understand the transient process of the induced current.

We again use the free-string model of the bunched beam. In this model the interaction of betatron and synchrotron oscillation is expressed explicitly by modulation of the betatron oscillation phase. But it does not include the circulation of the particles due to the synchrotron motion, which is essential to the head-tail instability; the increased amplitude of the tail particles is brought to the head by the circulation. In order to overcome this defect of the model, we make a new approach for the description of the instability; we calculate the average increase of the betatron oscillation amplitude over the string in one revolution period. When the growth rate of the instability is slow enough compared with the synchrotron oscillation, we expect that the betatron oscillation amplitude, being disturbed by the kick of the induced current, is continuously averaged by the circulation. Consequently, the current is always induced by the normal distribution of the betatron oscillation amplitude. The observed build-up time is 3 to 5 msec, while the synchrotron frequency is 3 to 10 kHz.

In the following we give the transient process of the induced current in Section 2. The free-string model is explained in Section 3, and the theory of the instability with the new approach is described. It is shown that in the limit of small chromaticity the theory leads to the Pellegrini-Sands formula of the growth rate.[2,3] Section 4 gives numerical results of the theory, which explain very well the experimental results. Finally, some discussions are given in Section 5 concerning the threshold of the instability.

2. TRANSIENT PROCESS OF INDUCED CURRENT

The matched kicker magnet is equivalently represented by an infinitely long LCR ladder network, a part of which is coupled with the beam current through the mutual inductance as shown in Fig. 1. We neglect the reflection of the induced current at the end of the long power cable. When a step-up current passes through the gap of the magnet, an equal ring current is induced almost instantaneously and simultaneously in every mesh of the network since the boundary condition of the magnet is unconstrained. The electromotive force is the same in every mesh; the band width is large enough and the magnet is short. The series of ring currents now begins to travel in both directions with constant velocity. The travel time through the magnet is given by

$$\tau_0 = N\sqrt{LC} \approx 42 \text{ nsec}, \qquad (2\text{-}1)$$

where $N(=12)$ is the number of mesh points in the magnet, and $L(=7.85\times10^{-8}\text{H})$ and $C(=155\times10^{-12}\text{F})$ are the inductance and capacitance per mesh respectively. Then the total amount of the ring currents still remaining in the magnet decreases linearly to zero in the travel time. In other words, the average current which remains in the magnet decreases as

$$\Psi(\Delta t) = \begin{cases} 1 - \dfrac{\Delta t}{\tau_0} & \text{for } 0 \le \Delta t \le \tau_0 \\ 0 & \text{otherwise} \end{cases} \qquad (2\text{-}2)$$

The measured travel time is approximately 50 nsec. Compared with the instability, we have the revolution period $T \simeq 200$ nsec and the bunch length $\tau \simeq 80$ nsec. Thus only the intra-bunch interaction works.

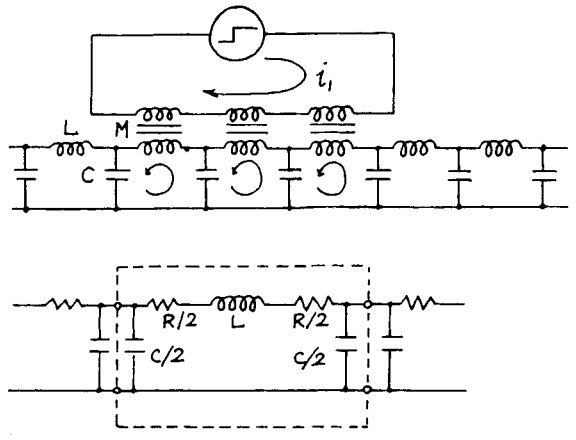

FIGURE 1 Equivalent circuit of a matched kicker magnet. A symmetric picture of one mesh is shown in the bottom.

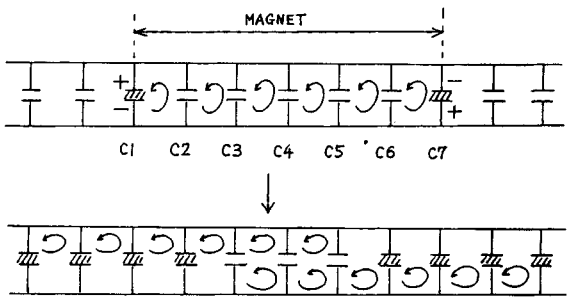

FIGURE 2 Transient process of the induced currents and the induced voltage which appears in the shaded capacities.

The above picture of the induced current was confirmed by observing the induced voltage at several capacitive electrodes of the magnet for a step-up current passing in a wire through the gap. At the instant when the ring currents are induced, a voltage is induced only at the electrodes at the magnet ends, because electric charge is stored there but not at the other electrodes. The ring currents travel in both directions; the inner electrodes are charged in turn as shown in Fig. 2. Hence the time dependence of

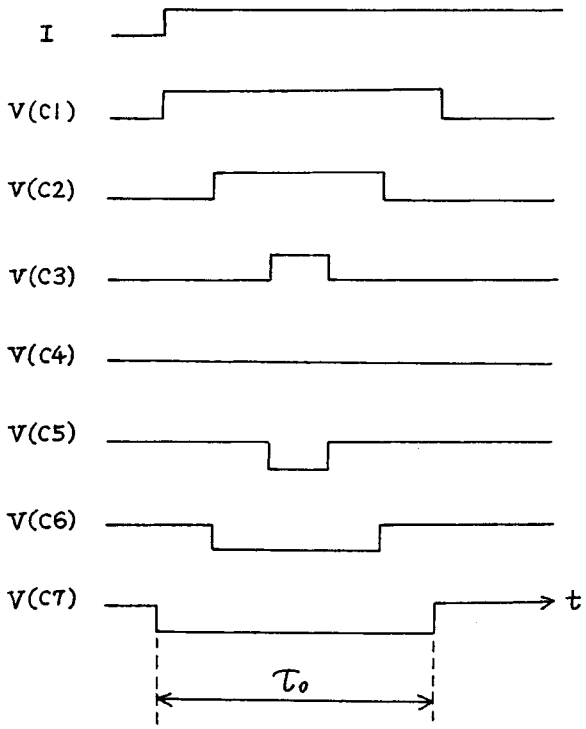

FIGURE 3 Expected time dependence of the induced voltage at capacitive electrodes.

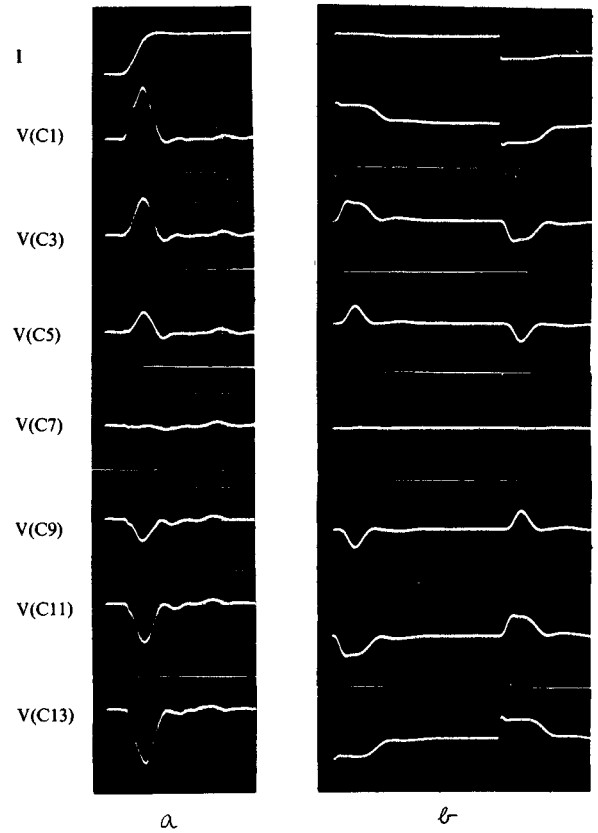

FIGURE 4 Observed time dependence of the induced voltage at the electrodes: a) the matched kicker magnet (100 nsec/div), b) the equivalent circuit with $L = 140\ \mu H$, $C = 0.057\ \mu F$, and $N = 12$ (20 μsec/div).

the induced voltage at the several electrodes is expected to be as shown in Fig. 3. Experimental results are shown in Fig. 4(a), which is not clearly the same, however, because of the slow rise of the passing current. Figure 4(b) is the induced voltage observed in an equivalent circuit made of electric parts whose L and C are large enough to give a relatively fast rise. This is close to Fig. 3.

3. THEORY OF THE HEAD–TAIL INSTABILITY

3.1 Free-String Model

In Ref. 10 we have explained the physical meaning of the free-string model of a bunched beam. Here we will make the model clearer by drawing the dynamic motion of the string and indicate the time variable that is seen by the magnet.

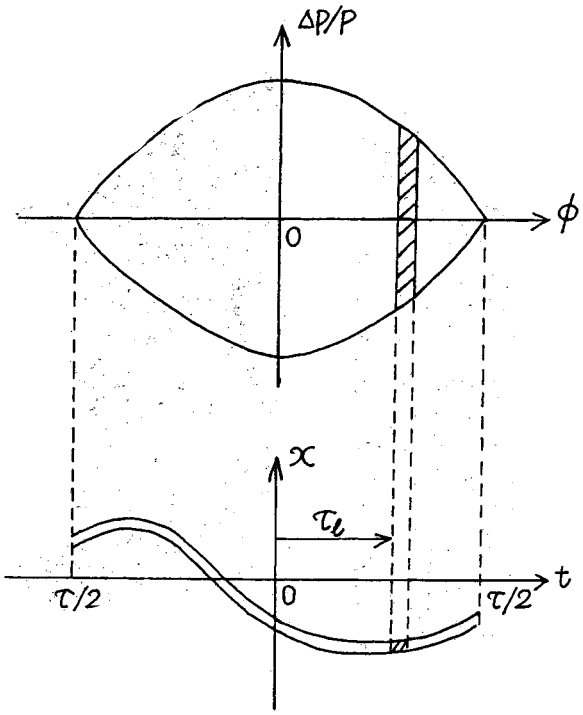

FIGURE 5 Free string model of a bunched beam.

The betatron amplitude of the l-th particle in a bunch is given by[3,10]

$$x_l = Z_l e^{i[\omega_\beta t + (\omega_\zeta - \omega_\beta)\tau_l(t)]} \tag{3-1}$$

where Z_l is the oscillation amplitude, ω_β the betatron frequency, ω_ζ is the chromatic frequency, and τ_l the time of arrival at a given point in the ring. So far as the coherent motion of many particles is concerned, x_l and Z_l can be regarded as the average of many particles that arrive at the same time τ_l at a given point (see Fig. 5). Then we can neglect the synchrotron oscillation of $\tau_l(t)$ but still keep the effect in the phase shift $(\omega_\zeta - \omega_\beta)\tau_l$. Now we put $t = kT + \tau_l$, where k is an integer and T the revolution period of the beam. Then

$$x_l = Z_l e^{i(\omega_\beta kT + \omega_\zeta \tau_l)}. \tag{3-2}$$

This expression was first given by Sacherer.[4]

Figure 6(a) illustrates the dynamic motion of the string expressed by Eq. (3-2) for $\omega_\zeta\tau = 2\pi$ and 0, where τ is the bunch length. The solid line indicates the string motion that will be observed at a given point. The broken line indicates the betatron motion of the head and tail. In fact these

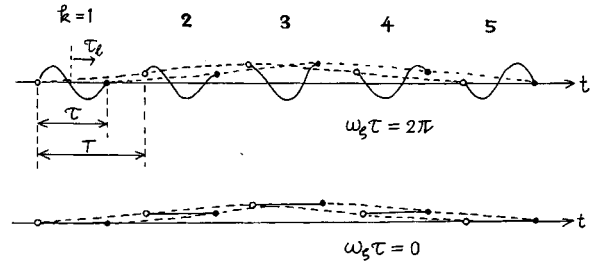

FIGURE 6-a Dynamic motion of a bunched beam observed at a given point in the ring.

bunch motions have been observed with more modulation from oscillation modes and charge distribution in the bunch.[5,9,10] In the kicker magnet, the current is induced through the mutual inductance. Therefore, the time variation of the passing current determines the induced current. So far as the intra-bunch interactions are concerned, τ_l should be taken as the time variable, as can be seen from the figure.

Figure 6(b) shows the string of motion in a system moving with the string or the betatron motion itself. The broken lines indicate the string motion seen at a given point in the ring. We see that the betatron oscillation trajectory for $\omega_\zeta\tau = 0$ is the only one, that is, every part of the string follows the trajectory of the head, and that the phase shift $x\ (= \omega_\zeta\tau)$ from head to tail is the phase difference of the betatron trajectories between the head and tail.

3.2 Formalism of the Growth Rate

As described in Section 1, the string model does not explicitly present the circulation of the par-

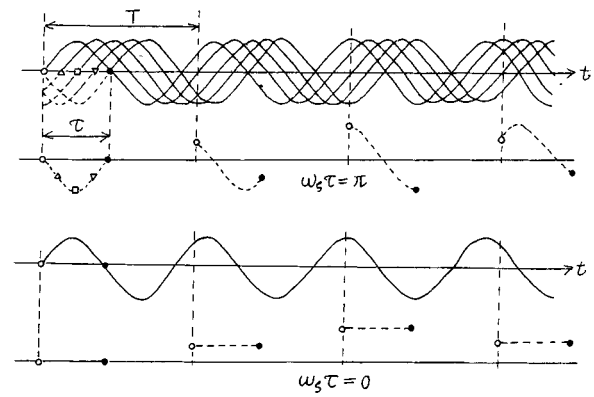

FIGURE 6-b Betatron-oscillation trajectory of several parts of a bunched beam. The dotted lines are the dynamic motion observed at a given point.

ticles due to the synchrotron motion; therefore, without some assumptions the amplitude of the tail would grow larger while that of the head remains small. We now consider the situation where the growth rate of the oscillation amplitude is slow compared with the synchrotron oscillation. Then we expect that the particles redistribute in one revolution after the kick to take almost the same amplitude A_m (which is given below) throughout the beam. Accordingly we assume that the current is always induced by the beam given by Eqs. (3-2) and (3-3), with A_m independent of τ_l.

Let us consider the betatron motion of the s-th part of the string in the phase space. Since τ_s ranges over $-\tau/2 \le \tau_s \le \tau/2$, the amplitude Z_s can be expressed by the summation of the normal modes. For simplicity, we consider only one term,

$$Z_s = A_m \cos m\omega_1\tau_s \text{ or } B_m \sin m\omega_1\tau_s, \quad (3\text{-}3)$$

where the integer m represents the mode number and $\omega_1 \equiv 2\pi/\tau$. For the present we consider the cosine mode. Now define S_0 in the phase space

$$S_0^2 \equiv (\mathrm{Re}\,[x_s])^2 + (\mathrm{Re}\,[\dot{x}_s/\omega_\beta])^2, \quad (3\text{-}4)$$

where $\mathrm{Re}\,[\dot{x}_s]$ means the real part of x_s and $\dot{x}_s = dx_s/dt'$. Because $t' \approx kT$ in Eq. (3-4), we find

$$S_0^2 = A_m^2 \cos^2 m\omega_1\tau_s. \quad (3\text{-}5)$$

Taking the average over $-\tau/2 \le \tau_s \le \tau/2$, we find

$$\sqrt{\langle S_0^2\rangle_{\tau_s}} = \begin{cases} A_m/\sqrt{2} & \text{for } m \neq 0 \\ A_0 & \text{for } m = 0 \end{cases} \quad (3\text{-}6)$$

If the beam is kicked once by a small amount $\Delta\dot{x}_s$, then

$$S_1^2 = (\mathrm{Re}\,[x_s])^2 + (\mathrm{Re}\,[(\dot{x}_s + \Delta\dot{x}_s)/\omega_\beta])^2. \quad (3\text{-}7)$$

Therefore

$$\sqrt{\langle S_1^2\rangle_{\tau_s}} \simeq \frac{A_m}{\sqrt{2}} - \frac{\sqrt{2}}{\omega_\beta}\langle \cos m\omega_1\tau_s \sin(\omega_\beta t' + \omega_\zeta\tau_s)\,\mathrm{Re}\,[\Delta\dot{x}_s]\rangle_{\tau_s}. \quad (3\text{-}8)$$

Taking into account Eq. (3-6), we set (see Fig. 7)

$$\sqrt{\langle S_1^2\rangle_{\tau_s}} = (A_m + \Delta A_m)/\sqrt{2}. \quad (3\text{-}9)$$

Hence

$$\Delta A_m \simeq -\frac{2\lambda}{\omega_\beta}\langle \cos m\omega_1\tau_s \sin(\omega_\beta t' + \omega_\zeta\tau_s)\,\mathrm{Re}\,[\Delta\dot{x}_s]\rangle_{\tau_s}.$$

$$\lambda \equiv \begin{cases} 1 & \text{for } m \neq 0 \\ \tfrac{1}{2} & \text{for } m = 0 \end{cases} \quad (3\text{-}10)$$

The quantity ΔA_m is the increase of the oscillation amplitude per kick or per revolution. If $\mathrm{Re}\,[\Delta\dot{x}_s]$ is proportional to A_m, we have an exponential increase of the amplitude because we have

$$\frac{dA_m}{dt'} \simeq \frac{\Delta A_m}{T} \simeq \beta_m A_m. \quad (3\text{-}11)$$

The growth rate is given by

$$\beta_m \simeq -\frac{2\lambda}{\omega_\beta T}\langle \cos m\omega_1\tau_s \sin(\omega_\beta t' + \omega_\zeta\tau_s)\,\mathrm{Re}\,[\Delta\dot{x}_s/A_m]\rangle_{\tau_s}. \quad (3\text{-}11')$$

This is the basic formula of the instability and indicates that in Eq. (3-11'), β_m is determined by the phase relation among several terms. The

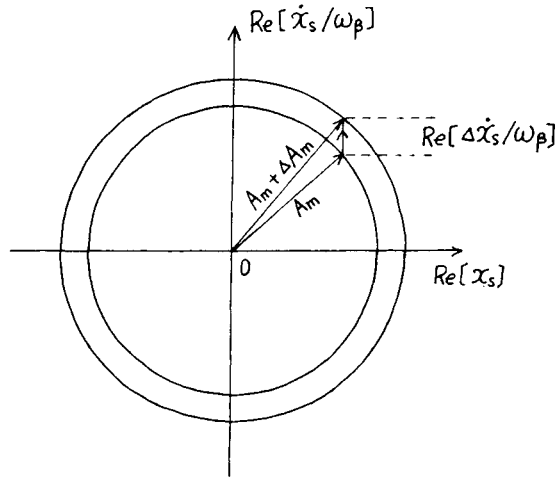

FIGURE 7 Betatron-oscillation trajectories in the phase space; one is before the kick and the other is after the kick.

build-up time is defined by $\tau_\gamma = 1/\beta_m$. Negative β_m gives coherent damping of the betatron oscillation.

3.3 Induced Current by Bunched Beam

Now we consider the current which is induced in the magnet by the l-th part of the beam whose horizontal position is given by Eqs. (3-2) and (3-3). Assume the following current distribution in the bunch

$$i_l = i_0 \cos \frac{\omega_1 \tau_l}{2} \quad (\omega_1 = 2\pi/\tau). \tag{3-12}$$

The beam current produces magnetic flux ϕ_l ($= Mi_l$) within the one-turn coil of the magnet and induces the secondary current. The induced current at the n-th mesh follows the equation[10]

$$\Omega^2(I_{n-1} + I_{n+1} - 2I_n) - \delta \dot{I}_n - \ddot{I}_n = -\ddot{\phi}_l/L, \tag{3-13}$$

where $\Omega = 1/(LC)^{1/2}$, $\delta = R/L$ and the time variable is τ_l as explained previously. Since the magnet length is short compared with the betatron wave length and also with the bunch length, and because of the matched boundary condition, the same amount of ring current is induced in every mesh at the instant when the l-th part passes through the magnet. Hence Eq. (3-13) reduces to

$$\ddot{I}_n + \delta \dot{I}_n = \ddot{\phi}_l/L. \tag{3-14}$$

Combining Eqs. (1-1), (3-2), (3-3), and (3-12), we find for the a and b terms of M

$$\left(\frac{\partial^2 \phi_l}{\partial \tau_l^2}\right)_a = -\sum_{\pm} \frac{a i_0}{2} \left(\frac{\omega_1}{2}\right)^2 e^{\pm i \frac{\omega_1}{2} \tau_l}$$
$$\left(\frac{\partial^2 \phi_l}{\partial \tau_l^2}\right)_b = \sum_{\pm} \frac{A_m b i_0}{4} \Omega_m{}^{\pm 2} e^{i\Omega_m{}^{\pm} \tau_l} e^{i\omega_\beta \tau'}, \tag{3-15}$$

where $\Omega_m{}^{\pm} = \omega_\zeta \pm (m \pm \frac{1}{2})\omega_1$ and $\sum_{\pm}$ means the sum over every combination of + and − sign. Inserting these into Eq. (3-14), we find for the induced current due to the l-th part of the beam

$$I_l = \sum_{\pm} \frac{a i_0}{2L} D_m{}^{\pm} e^{i\theta_m{}^{\pm}} e^{\pm i(\omega_1/2)\tau_l} - \sum_{\pm} A_m e^{i\omega_\beta t'} \frac{b i_0}{4L} D_m{}^{\pm} e^{i\theta_m{}^{\pm}} e^{i\Omega_m{}^{\pm} \tau_l}, \tag{3-16}$$

where

$$D_m{}^{\pm} = [1 + (\delta/\Omega_m{}^{\pm})^2]^{-1/2}$$
$$\theta_m{}^{\pm} = \arctan(\delta/\Omega_m{}^{\pm}) \tag{3-16'}$$
$$\Omega_m{}^{\pm} = \begin{cases} \omega_\zeta \pm (m \pm \frac{1}{2})\omega_1 & \text{for the } b\text{-term} \\ \pm(\frac{1}{2})\omega_1 & \text{for the } a\text{-term} \end{cases}$$

The factor $\delta (= R/L)$ depends strongly on the relevant frequency, which is now $\Omega_m{}^{\pm}$. The experimental value of R is given in Appendix I. The cutoff frequency of the network is about 90 MHz.

3.4 Growth Rate of the Instability

The series of ring currents induced by the l-th part travels away out of the magnet with the reduction rate $\bar{\psi}(\Delta t)$. The ring currents still remaining in the magnet produce magnetic field vertically in the gap. The average field is given by

$$B_l(\Delta t) = \frac{\mu_0}{h} I_l \bar{\psi}(\Delta t), \tag{3-17}$$

where h is the gap height of the magnet. This field exerts forces on the s-th part of the beam, which arrives at the magnet later than the l-th part. Taking into account the direction of the force we find for the kick of the s-th part

$$\Delta \dot{x}_s = -\frac{e l_B}{m_0 \gamma} \sum_{l}^{l<s} B_l(\tau_{sl}), \tag{3-18}$$

where e is the electric charge, l_B the magnet length, m_0 the proton rest mass, γ the relativistic energy and $\tau_{sl} = \tau_s - \tau_l$. The summation $\sum_l^{l<s}$ means the contribution of all the parts that preceed the s-th part.

For the present we consider only the b term of Eq. (3-16). Then

$$\Delta \dot{x}_s = -\frac{e l_B}{M_0 \gamma} \frac{\mu_0}{h} \frac{b i_0}{4L} A_m e^{i\omega_\beta t'} \times \sum_{\pm} D_m{}^{\pm} e_l^{i\theta_m{}^{\pm}} \sum_{l}^{l<s} e^{i\Omega_m{}^{\pm} \tau_l} \bar{\psi}(\tau_{sl}). \tag{3-19}$$

The summation over l up to s is obtained by the following integration,

$$\sum_{l}^{l<s} = \frac{1}{\tau} \int_{-\tau/2}^{\tau_s} e^{i\Omega_m{}^{\pm} \tau_l} \bar{\psi}(\tau_{sl}) d\tau_l$$

$$= \left[\frac{1}{i\Omega_m{}^{\pm}\tau} \left\{ 1 - \left(1 - \frac{t''}{\tau_0} \right) e^{-i\Omega_m{}^{\pm} t''} \right\} + \frac{}{\Omega_m{}^{\pm}\tau_0\tau} \left(1 - e^{-i\Omega_m{}^{\pm} t''} \right) \right] e^{i\Omega_m{}^{\pm}\tau_s}$$

$$\equiv G\, e^{i\phi} e^{i\Omega_m{}^{\pm}\tau_s}, \tag{3-20}$$

where

$$t'' = \begin{cases} \tau_s + \tau/2 & \text{for} \quad -\tau/2 \le \tau_s \le \tau_0 - \tau/2 \\ \tau_0 & \text{for } \tau_0 - \tau/2 \le \tau_s \le \tau/2 \end{cases}$$

Now we are ready to calculate the growth rate with the basic formula Eq. (3-11). First we note that $\Delta\dot{x}_s$ is proportional to A_m as seen in Eq. (3-19). The real part of $\Delta\dot{x}_s$ is given by

$$\mathrm{Re}\,[\Delta\dot{x}_s] \propto \cos(\omega_\beta t' + \Omega_m{}^{\pm}\tau_s + \theta_m{}^{\pm} + \phi). \tag{3-21}$$

Multiplying this by $\sin(\omega_\beta t' + \omega_\zeta\tau_s)$, we find

$$\mathrm{Re}\,[\Delta\dot{x}_s] \propto \tfrac{1}{2}\{\sin(2\omega_\beta t' + \omega_\zeta\tau_s + \Omega_m{}^{\pm}\tau_s + \theta_m{}^{\pm} + \phi) + \sin(\omega_\zeta\tau_s - \Omega_m{}^{\pm}\tau_s - \theta_m{}^{\pm} - \phi)\}. \tag{3-21'}$$

The first term varies sinusoidally with time and its time average cancels to zero, but the second term remains. Hence we derive finally the formula of the growth rate

$$\beta_m = -\lambda H \sum_{\pm} D_m{}^{\pm} \langle G \cos m\omega_1\tau_s \sin[\pm(m \pm \tfrac{1}{2})\omega_1\tau_s + \theta_m{}^{\pm} + \phi] \rangle_{\tau_s}, \tag{3-22}$$

where H is defined by

$$H = \frac{1}{16}\frac{e^2}{m_0\gamma}\frac{\mu_0 b l_B}{hL}\frac{N_0}{\nu\tau} = 7.63 \times 10^{-5}/\nu\gamma\tau \quad \text{for } N_0 = 4.0 \times 10^{11}. \tag{3-23}$$

We have used the relation $i_0 = \pi e N_0/2\tau$ for the current distribution Eq. (3-12); N_0 is the number of particles in the bunch. The chromaticity dependence appears through G and ϕ defined in Eq. (3-20), and this formula covers a wide range of chromaticity.

We have derived a formula for the b-term of M. The a-term contribution cancels in the many-turn average, because the induced current due to the a-term does not include the factor $e^{i\omega_\beta t'}$ [see Eq. (3-16)]. Therefore $\sin(\omega_\beta t' + \omega_\zeta\tau_s)$ remains in the final form of β_m.

So far we have considered the cosine mode of Eq. (3-3). The sin mode gives a similar result

$$\beta_m(\sin) = -\lambda H \sum_{\pm} p D_m{}^{\pm} \langle G \sin m\omega_1\tau_s \times \sin[p(m \pm \tfrac{1}{2})\omega_1\tau_s + \theta_m{}^{\pm} + \phi] \rangle_{\tau_s} \tag{3-24}$$

where p takes + and − signs.

3.5 Derivation of Pellegrini-Sands Formula

Before performing a numerical calculation of the growth rate, we consider a simplified case of the preceeding discussion, and will derive the Pellegrini-Sands formula of the head-tail instability in the limit of small chromaticity.

Let us consider the cosine mode and go back to Eqs. (3-19) and (3-11). Assume $R = 0$ or no loss. Then $D_m{}^{\pm} = 1$ and $\theta_m{}^{\pm} = 0$. Then

$$\beta_m = \lambda H \left\langle \sum_{\pm} \sum_{l}^{l<s} \cos m\omega_1\tau_s \sin(\omega_\beta t' + \omega_\zeta\tau_s) \times \cos(\omega_\beta t' + \Omega_m{}^{\pm}\tau_l)\, \bar{\psi}(\tau_{sl}) \right\rangle_{\tau_s}. \tag{3-25}$$

The summation $\pm$ and many-turn average lead to

$$\beta_m = \lambda H \left\langle \sum_{l}^{l<s} \cos m\omega_1\tau_s \cos m\omega_1\tau_l \sin\omega_\zeta(\tau_s - \tau_l) \times \cos\frac{\omega_1}{2}\tau_l\, \bar{\psi}(\tau_{sl}) \right\rangle_{\tau_s} \tag{3-26}$$

This expresses straightforwardly the meaning of each term. Hence for the sine mode we only need to change $\cos(m\omega_1\tau_s)\cos(m\omega_1\tau_l)$ to $\sin(m\omega_1\tau_s)\sin(m\omega_1\tau_s)$.

We further assume a constant current distribution ($\cos\omega_1/2\,\tau_l \to 1$) and a sufficiently slow decay [$\bar{\psi}(\tau_{sl}) \to 1$], but no effect on the next turn. Then summation over l in Eq. (3-26) gives

$$\sum_{l}^{l<s} \sin\omega_\zeta(\tau_s - \tau_l)\cos m\omega_1\tau_l$$

$$= \sum_{\pm} \frac{1}{2} \frac{-1}{(\omega_\zeta \pm m\omega_1)\tau} \left\{ \cos m\omega_1 \tau_s - \cos\left[(\omega_\zeta \pm m\omega_1) \frac{\tau}{2} + \omega_\zeta \tau_s \right] \right\}. \tag{3-27}$$

By averaging over τ_s, we find

$$\beta_m = 2\lambda H \frac{\omega_\zeta/\tau}{(m\omega_1)^2 - \omega_\zeta^2} \left\{ \left(\frac{1}{2}\right)^* + \frac{\omega_\zeta^2}{(m\omega_1)^2 - \omega_\zeta^2} \frac{\sin \omega_\zeta \tau}{\omega_\zeta \tau} \right\}, \tag{3-28}$$

where $(\frac{1}{2})^*$ should be replaced by 1 for $m = 0$. In the limit of $\omega_\zeta \tau \ll 1$,

$$\beta_0 \approx -\frac{H}{6} \omega_\zeta \tau \qquad (m = 0)$$
$$\beta_m \approx \frac{H}{(2m\pi)^2} \omega_\zeta \tau \quad (m \neq 0). \tag{3-29}$$

Therefore for negative $\omega_\zeta (= \zeta/\eta\, \omega_\beta)$, where ζ is the chromaticity $\eta = \alpha - 1/\gamma^2$ and α is the momentum compaction factor, the mode $m = 0$ is unstable and other modes are stable, and vice versa for positive ω_ζ. These are very close to the formula of the head-tail effect derived by Pellegrini and Sands

$$\beta_m = \frac{2}{\pi^2} \frac{N_0 SA}{\alpha} \frac{\zeta}{4m^2 - 1}, \tag{3-30}$$

where S is the wake force per unit deviation divided by $m_0\gamma$ and $A = \tau/2$. Comparing Eqs. (3-29) and (3-30) for $m \neq 0$ we expect to have the relation

$$m_0 \gamma S \approx f \frac{\Delta\tau}{2\tau}, \tag{3-31}$$

where $\Delta\tau \equiv l_B/v$ is the passing time of a part of the beam through the magnet and $f \equiv evB$ with $B \approx \mu_0$, be/hLT. The right-hand side means approximately the average force in one revolution, which is in accord with the definition of S. The results of numerical calculation of Eq. (3-28) or more generally of Eq. (3-26) with some decay function $\bar{\psi}(\tau_{sl})$ will be given in Appendix II.

4. NUMERICAL CALCULATION AND COMPARISON WITH EXPERIMENTS

We calculate numerically the growth rate of the instability with the formulas of Eqs. (3-22) and (3-24), and will show that the results agree well with the experiments, which are summarized as follows:[9]

1. Build up time is 3 to 5 msec,
2. Instability is induced around 13 to 20 msec after injection of the beam,
3. Threshold beam intensity is approximately $N_0 \approx 3 \times 10^{11}$,
4. Only the mode $m = 0$ has been observed,
5. In spite of the instability, the horizontal emittance of the extracted beam does not seem to be increased,
6. Instability is suppressed by decreasing the chromaticity close to zero and also by increasing it by about the same amount,
7. Instability is suppressed by applying a small amount of octupole correction field.

Items 3 and 7 are related to tune spread of the betatron oscillation, which has not taken into account in the above discussion.

For the numerical calculation of Eqs. (3-22) and (3-24), we need numerical values of $D_m^{\pm}$ and $\theta_m^{\pm}$, which are given in Appendix I, and of T, τ, γ, ν, and ζ during the acceleration, which are given in Ref. 10. We only note that ζ is positive (≈ 0.4) at first, decreases to zero at 20 msec after the injection because of the saturation of the magnetic field, and then goes negative and that η is negative, hence the chromatic frequency ω_ζ changes sign from negative to positive at 20 msec. Three identical kicker magnets are installed in the ring, so that β_m of Eqs. (3-22) and (3-24) should be multiplied by 3. The calculations are made for $N_0 = 4 \times 10^{11}$.

Figure 8 gives the numerical results of β_m for cosine and sine modes, which explain items 1, 2, 4, and 5. The β_0 for cos-mode $m = 0$ becomes maximum around 17 msec, and the buildup time is $\tau_\gamma \approx 5$ msec. The β_m for other modes are small. The β_m for every mode becomes zero at 20 msec when the chromaticity is zero; β_0 decreases rapidly after 18 msec and becomes large and negative. This means that the amplitude coherently increased by the instability damps coherently just after the instability, resulting in no emittance growth. Figure 9 is $q(= \zeta\nu/\eta)$ dependence of β_m

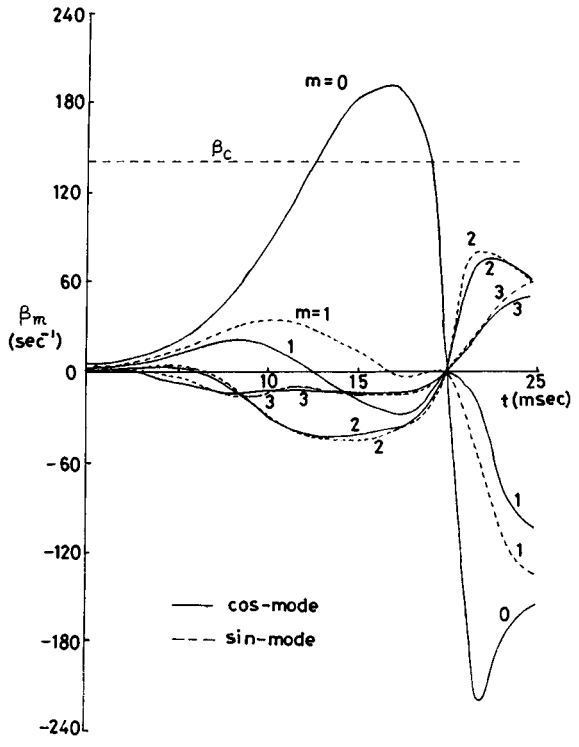

FIGURE 8 Growth rate of the instability during acceleration.

for cos and sin mode at 16 msec after the injection, which explains item 6. In the normal operation we have $q = -1.5$ around 16 msec, which is close to the point of maximum β_0. Increase and decrease of q give lower β_0. Instability has been observed only above a beam intensity $N_0 \approx 3 \times 10^{11}$ which gives a critical growth rate $\beta_c \simeq 140\ \text{sec}^{-1}$, shown with a broken line in Fig. 8 and Fig. 9. Hence the unstable region is 13 to 19 msec in Fig. 8 and $q = -4.0$ to -1.0 in Fig. 9. The growth rates for $m \neq 0$ are all lower than β_c. Relation between the critical rate and the tune spread will be discussed in Section 5.

The effect of the magnet loss on the instability is found to be negligible, because the growth rate calculated for $R = 0$ is almost the same as the previous ones. This is because the relevant frequency close to the instability is $|\Omega_m^{\pm}| \leq 30$ MHz for the mode $m = 0$, 1, and 2. Therefor the phase shift $\theta_m^{\pm}$ is at most 15 degrees and $D_m^{\pm} \approx 1$ as seen in Fig. A-2.

The traveling time or decay constant of the induced current does not play a critical role for the instability. Figure 10 shows β_0 for various τ_0 calculated on the assumption that only intra-bunch interaction affects the motion. Then β_0

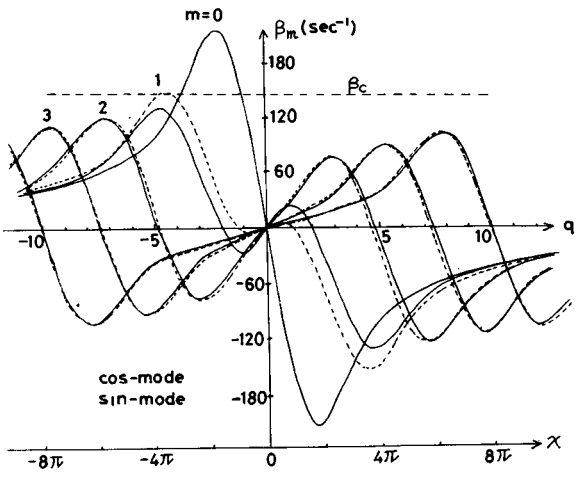

FIGURE 9 Chromaticity dependence of the growth rate at 16 msec, $q = \zeta\nu/\eta$.

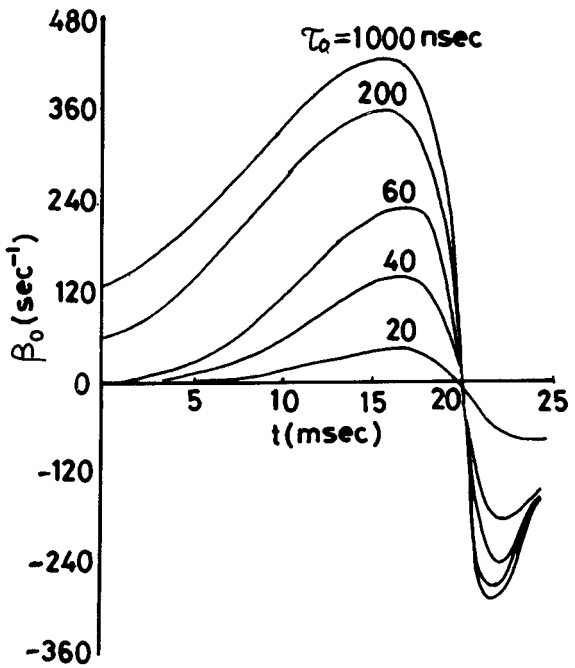

FIGURE 10 Traveling time dependence of the growth rate for $m = 0$.

monotonically increases with τ_0 and saturates for $\tau_0 \gtrsim 3\tau$.

5. DISCUSSION

We consider the effect of the tune spread on the coherent instability in connection with items 3 and 7. The coherent betatron oscillation competes with the phase compensation due to the tune spread. We expect the instability would be suppressed by the presence of the tune spread

$$\Delta\nu \approx T/\tau_\gamma \approx 3 \times 10^{-5} \qquad (5\text{-}1)$$

Indeed it was suppressed by an correction octupole field $B''' l_0 \simeq \pm 20\ T/m^2$, which introduces a momentum-independent tune spread $\Delta\nu \approx 2 \times 10^{-5}$ in accord with Eq. (5-1). The threshold beam intensity gives a critical buildup time $\tau_{\gamma c} \approx 7$ msec. This implies that the machine has a built-in tune spread of the order of 10^{-5}, which is extremely small. On the other hand, the momentum-dependent tune spread is about 1×10^{-3}. We should notice, however, that this tune spread does not contribute to the phase compensation. Instead it introduces the chromatic phase shift given by Eq. (3-1). In other words, this tune spread is coherently related to the betatron oscillation and promotes the instability.

ACKNOWLEDGEMENTS

The author would like to express his sincere thanks to Dr. A. G. Ruggiero for his stimulating discussion and also to the Fermi National Accelerator Laboratory for its hospitality during his stay at the Laboratory.

REFERENCES

1. E. D. Courant and A. M. Sessler, Rev. Sci. Instrum. 37, 1579 (1966).
2. C. Pellegrini, Nuovo Cimento 64A, 477 (1969).
3. M. Sands, SLAC-TN-69/8 and SLAC-TN-69/10 (1969).
4. F. Sacherer, Proceedings from the 9th International Conf. on High Energy Accelerators, Stanford, 347 (1974).
5. J. Gareyte and F. Sacherer, ibid 341.
6. D. Möhl, MPS/DL/Note 74-6.
7. H. H. Umstatter, MPS/SM/Note 74-15.
8. B. Zotter, CERN/ISR-TH/78-16.
9. Y. Kimura, Y. Miyahara, H. Sasaki, K. Satoh, K. Takata, and K. Takikawa, Proceedings of the 10th International Conf. on High Energy Accelerators, Serpukhov, 2, 30 (1977).
10. Y. Miyahara and K. Takata, Particle Accelerators 10, 125 (1980).
11. G. Nassibian and F. Sacherer, CERN/ISR-TH/77-61.
12. Y. S. Derbenev, N. S. Dikansky, and D. V. Pestrikov, Particle Accelerators 8, 129 (1978).

Appendix I

The frequency dependence of the resistance R in the ladder network of the magnet was obtained by measurement of the Q-value of three resonance frequencies of the magnet without the matched resistance.[10] The resistance depends quadratically on the frequency, as shown in Fig. A-1. Assuming a constant L, we derive a frequency dependence $D(\omega) = 1/(1 + [\zeta(\omega)/\omega]^2)^{1/2}$ and $\theta(\omega)$ (= arctan $[\zeta(\omega)/\omega]$), shown in Fig. A-2. The frequency region is limited by a cutoff frequency. The matched kicker magnet can be regarded as an infinite series of a symmetric four part shown in Fig. 1. It is a low-pass filter and the cutoff frequency is given by

$$\omega_c = 2[(1 - CR^2/4L)/LC]^{1/2}$$

$$\approx 2\pi \times 90\ (\text{MHz}).$$

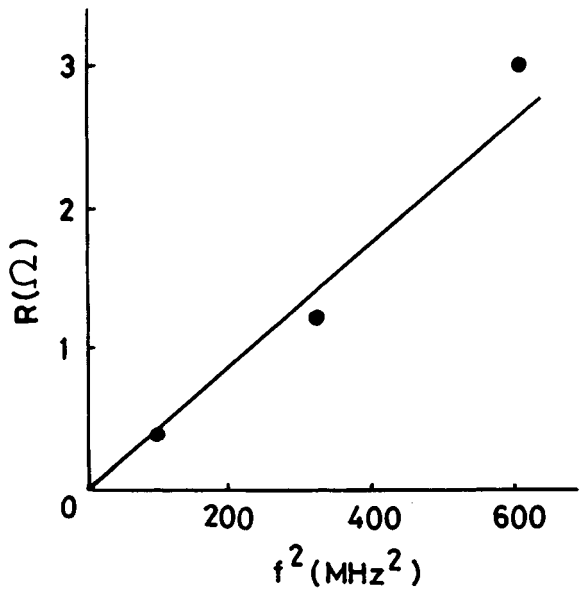

FIGURE A-1 Frequency dependence of the loss in the kicker magnet.

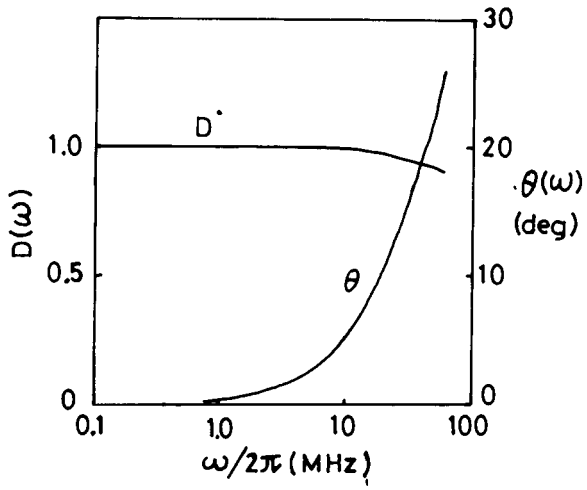

FIGURE A-2 Frequency dependence of $D_m^{\pm}(\omega)$ and $\theta_m^{\pm}(\omega)$.

Appendix II

For general purposes, we give here numerical results of the correlation function $F_m(\chi)$ of the growth rate $\beta_m = HF_m(\chi)$ for a lossless obstacle

$$F_m(\chi) \equiv 2\lambda \left\langle \sum_{l}^{l<s} \cos m\omega_1\tau_s \cdot \cos m\omega_1\tau_l \times \sin \omega_\zeta(\tau_s - \tau_l) \cdot \cos \frac{\omega_1}{2}\tau_l \cdot \bar{\psi}(\tau_{sl}) \right\rangle \tau_s,$$

where $\chi(= \omega_\zeta\tau)$ is the chromatic phase shift from head to tail. For the sin mode, $\cos m\omega_1\tau_s \cos m\omega_1\tau_l$ should be substituted for $\sin m\omega_1\tau_s \cdot \sin m\omega_1\tau_s$. Figure A-3 gives the results. The maximum values of $F_m(\chi)$ appear close to $|\chi| = (2m + 1)\pi$. Figure A-4 shows the τ_0 dependence of $F_m(\chi)$, where we have assumed $\bar{\psi}(\tau_{sl}) = \exp(-\tau_{sl}/\tau_0)$ with $\tau = 100$ msec.

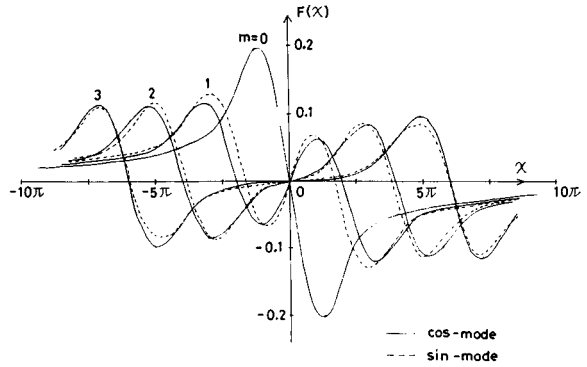

FIGURE A-3 Correlation function $F_m(\chi)$ as a function of chromatic phase shift χ.

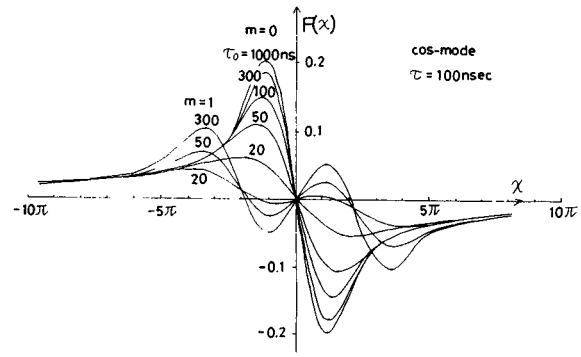

FIGURE A-4 Dependence of $F_m(\chi)$ on the damping time of the wake field.